

Multi-modality imaging: Bird's eye view from the 2018 American Heart Association Scientific Sessions

Mouaz H. Al-Mallah, MD, MSc, FASNC,^a Steven G. Lloyd, MD,^{b,c} Rami Doukky, MD, MSc, FASNC,^d Wael A. Aljaroudi, MD, FASNC,^e and Fadi G. Hage, MD, MASNC^{b,c}

^a Houston Methodist DeBakey Heart & Vascular Center, Houston Methodist Hospital, Houston, TX

^b Division of Cardiovascular Medicine, University of Alabama at Birmingham, Birmingham, AL

^c Birmingham Veterans Affairs Medical Center, Birmingham, AL

^d Cook County Health, Chicago, IL

^e Division of Cardiovascular Medicine, Clemenceau Medical Center, Beirut, Lebanon

Received Jan 7, 2019; accepted Jan 8, 2019

doi:10.1007/s12350-019-01603-4

This review summarizes key imaging studies that were presented at the American Heart Association Scientific Sessions 2018 in Chicago related to the fields of nuclear cardiology (including single photon emission computed tomography and positron emission tomography), cardiac computed tomography, cardiac magnetic resonance, and echocardiography. The aim of this bird's eye view is to inform readers of the various studies discussed at the meeting from these imaging modalities. While this review is directed to the benefit of those of us who were not able to attend the conference, we find that a general overview may also be useful to those that did since it is often difficult to get exposure to all abstracts at large meetings. Further, we hope that the presentation of multiple imaging studies in a single synthesized review will stimulate new ideas for future research in imaging. (J Nucl Cardiol 2019;26:645–54.)

Key Words: CAD • cardiomyopathy • sarcoid heart disease • PET • MRI • CT

Abbreviations

AHA 2018 American Heart Association Scientific Sessions
 CAC Coronary artery calcium
 CAD Coronary artery disease
 CCTA Coronary computed tomography angiography
 CD/MI Cardiac death or non-fatal myocardial infarction
 CFR Coronary flow reserve
 CMR Cardiac magnetic resonance

CRF Cardiorespiratory fitness
 CT Computed tomography
 FFR Fractional flow reserve
 LGE Late gadolinium enhancement
 LVEF Left ventricular ejection fraction
 MPI Myocardial perfusion imaging
 PCAT Peri-coronary adipose tissue
 PET Positron computed tomography
 SPECT Single photon emission computed tomography

Reprint requests: Fadi Hage, MD, MASNC, Division of Cardiovascular Medicine, University of Alabama at Birmingham, Lyons Harrison Research Building 306, 1900 University Blvd, Birmingham, AL 35294; fadihage@uab.edu

1071-3581/\$34.00

Copyright © 2019 American Society of Nuclear Cardiology.

This bird's eye view from the 2018 American Heart Association Scientific Sessions (AHA 2018) which was held in Chicago, Illinois from November 10 to 12 will review key abstracts presented at the meeting related to

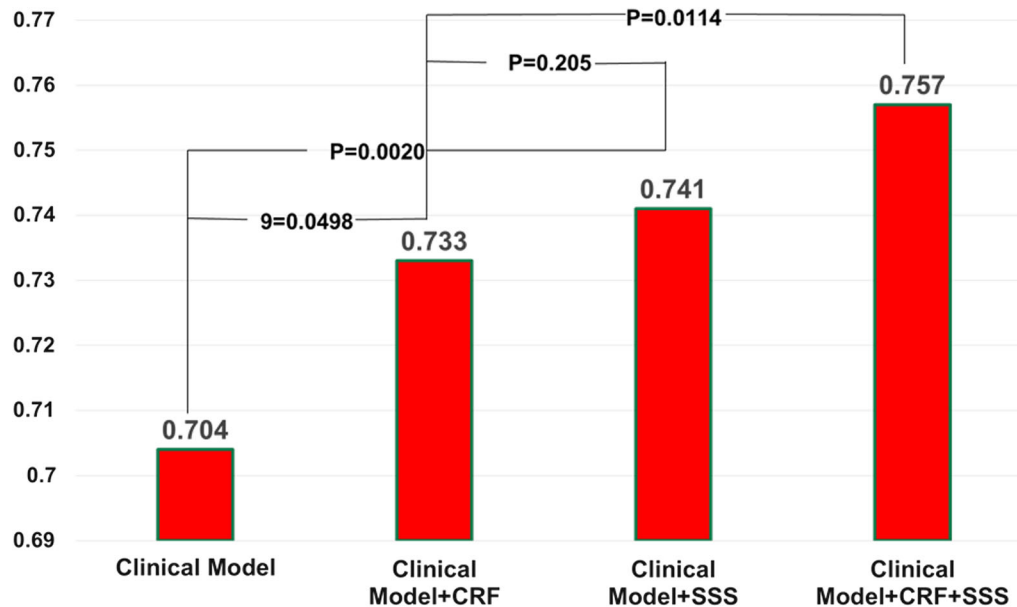


Figure 1. While both SPECT-MPI and CRF are independent predictors of major cardiac event, SPECT-MPI adds incremental prognostic value over CRF. Clinical Model includes age, gender, prior CAD, Hypertension, Diabetes, Cholesterol, Smoking, and eGFR.

imaging following a similar structure to our view from previous years.¹⁻⁴ This year we have dedicated a special section to positron computed tomography (PET) separate from the section on planar and single photon emission computed tomography (SPECT). We continue the tradition of summarizing studies in cardiac computed tomography (CT), cardiac magnetic resonance (CMR), and echocardiography. We acknowledge that no review can summarize all the imaging studies that are presented at a large conference of the magnitude of AHA 2018 but we hope that our review will be useful to the readers.

PLANAR AND SPECT

Several abstracts at AHA 2018 reported on investigations involving planar and SPECT imaging techniques. Saito et al⁵ studied the association between cardiac sympathetic nervous function and response to cardiac rehabilitation in patients with heart failure. The authors studied 35 patients with heart failure (mean left ventricular ejection fraction [LVEF] $46 \pm 20\%$, mean VO_2 max 14.5 ± 3.3 mL/min/kg) who underwent ^{123}I -metaiodobenzylguanidine imaging and cardiopulmonary exercise testing, and participated in a 3-month cardiac rehabilitation program. The study found that among responders to cardiac rehabilitation ($> 5\%$ increase in anaerobic threshold) heart-to-mediastinal ratio was significantly lower compared to non-responders

(1.80 ± 0.45 vs 2.37 ± 0.60 , $P < 0.05$) and washout rate of ^{123}I -metaiodobenzylguanidine was significantly higher in responders compared to non-responders ($39.7 \pm 7.4\%$ vs $31.2 \pm 9.0\%$, $P < .05$). The authors concluded that impaired cardiac sympathetic nervous function was closely correlated with a good response to cardiac rehabilitation in patients with heart failure.

Cantu et al⁶ investigated the association of exercise capacity, heart rate recovery, chronotropic incompetence, and all-cause mortality during exercise-myocardial perfusion SPECT in patients with left ventricular systolic dysfunction. During a median 13-year follow-up of 191 patients with systolic dysfunction (LVEF $< 50\%$) who underwent SPECT myocardial perfusion imaging (MPI), 78 deaths were observed. The SSS, impaired exercise capacity (< 7 METs), impaired heart rate recovery (≤ 22 bpm at 2 minutes), and chronotropic incompetence ($[\text{peak heart-rest heart}]/[220 - \text{age} - \text{rest heart rate}] < 0.8$) were associated with all-cause mortality. There was a stepwise increase in the risk of all-cause mortality with increasing number of abnormal exercise variables. In multivariable analysis, having 2 or 3 abnormal exercise variables was associated with increased risk of all-cause mortality (HR, 1.63; 95% CI 1.01-2.65; $P < .05$). Low exercise capacity was most strongly associated with all-cause mortality (HR, 1.89; 95% CI 1.13-3.18, $P = .01$). The authors concluded that in patients with systolic heart failure undergoing exercise SPECT-MPI, exercise capacity,

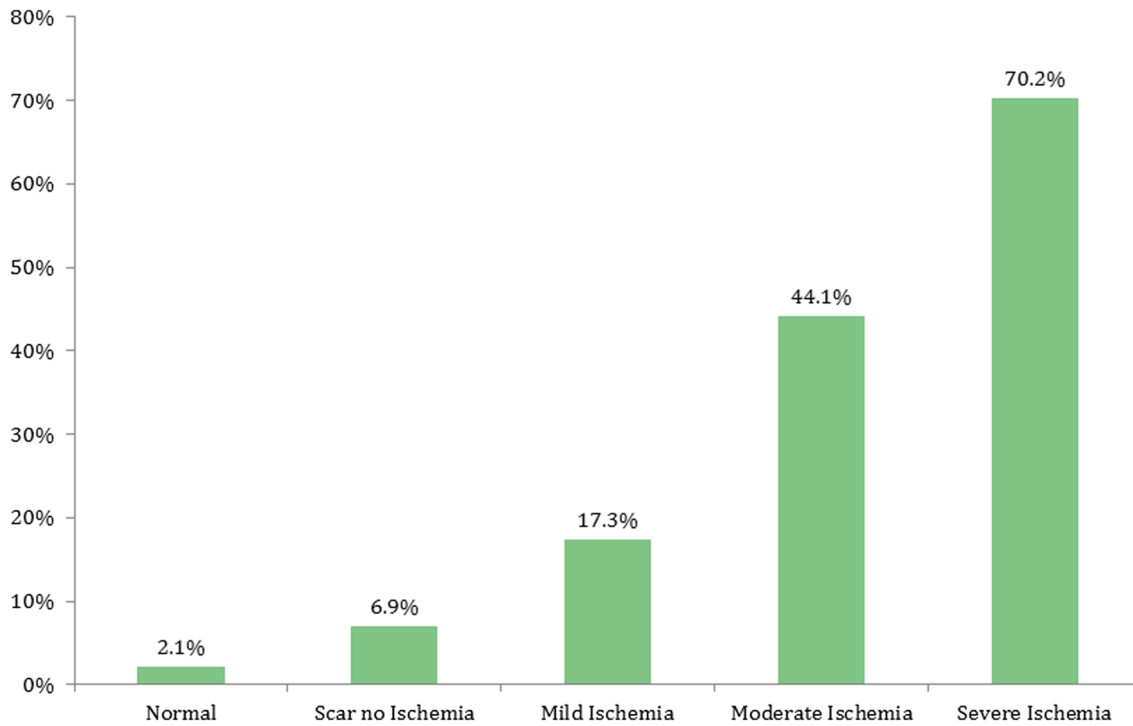


Figure 2. Rate of referral to coronary angiography post positron emission tomography myocardial perfusion imaging.

heart rate recovery, and chronotropic incompetence are independent predictors of all-cause mortality and add incremental value to MPI. Thus, when possible, exercise testing, providing these functional variables, would be preferable to pharmacologic testing for purposes of risk stratification.

Al Badarin et al⁷ investigated differences in post-test invasive angiography referral patterns between PET and SPECT. From a single-center cohort of 74,244 MPI studies of patients with or without coronary artery disease (CAD), the author propensity matched 25,868 MPI studies, equally split between SPECT and PET. A total of 3422 (13.2%) patients were referred to early angiography, within 90 days after MPI, (16.2% with PET vs 10.3% with SPECT; OR 1.51, 95% CI [1.39-1.64]; $P < .001$). At any level of ischemia, utilization of angiography post-MPI was higher with PET than SPECT. PET-determined ischemia was a more powerful predictor of early angiography (P for ischemia-modality interaction = 0.04). The authors concluded that in a contemporary, single-center cohort, early angiography rates were higher after PET compared to SPECT, and PET-derived ischemia was more strongly associated with angiography referral.

Al-Mallah et al⁸ investigated the incremental prognostic value of SPECT-MPI over cardiorespiratory

fitness (CRF). In a retrospectively cohort of 3216 patients referred for an exercise SPECT-MPI and followed for a median of 5.5 years, 150 (4.7%) subjects experienced cardiac death or non-fatal myocardial infarction (CD/MI). Using Cox regression, both CRF and MPI were independent predictors of outcomes. Compared to conventional risk factors alone, both CRF (AUC, 0.733 [95% CI 0.693-0.772] vs 0.705 [95% CI 0.663-0.746]; $P = .049$) and SPECT-MPI (AUC, 0.741 [95% CI 0.699-0.783] vs 0.704, [95% CI 0.662-0.746]; $P = .002$) improved prediction of CD/MI. However, SPECT-MPI added incremental prognostic value over CRF in predicting CD/MI (AUC, 0.757 [95% CI 0.716-0.797] vs 0.732 [95% CI 0.693-0.772], $P = .0114$), while CRF did not add over MPI (Figure 1). The authors concluded that while both SPECT-MPI and CRF are independent predictors of major cardiac event, SPECT-MPI adds incremental prognostic value to CRF.

In a sub-study of the PACIFIC-Trial, van Diemen et al⁹ investigated the impact of scan quality on the diagnostic performance of coronary CT angiography (CCTA), SPECT and PET for identifying myocardial ischemia as defined by a fractional flow reserve (FFR) of ≤ 0.80 . The authors analyzed 208 patients with suspected CAD, who underwent 256-slice CCTA, ^{99m}Tc-tetrofosmin SPECT, and [¹⁵O] H₂O PET prior

to invasive coronary angiography in conjunction with three-vessel FFR measurements. Scans were analyzed in core laboratories. Results are presented on a per patient level. The distribution of good, moderate, and poor-quality scans for CCTA was 137 (66%), 45 (22%), 27 (12%), respectively. The quality distribution for SPECT was 108 (52%), 79 (38%), 19 (10%), and for PET it was 175 (86%), 27 (13%), 2 (1%), respectively. Compared to moderate quality CCTA scans, high quality scans were associated with greater specificity (75% vs 31%, $P < .001$), positive predictive value [PPV] (71% vs 51%, $P = .050$), and accuracy (80% vs 68%, $P = .009$). Sensitivity or negative predictive value (NPV) of CCTA did not differ across scan quality groups. Sensitivity of good quality SPECT scans was superior to moderate (76% vs 41%, $P = .001$) and poor image quality scans (30%, $P = .003$). A similar trend was seen with regard to accuracy and NPV of SPECT. Scan quality did not influence diagnostic value of PET. A comparison of diagnostic performance of good quality CCTA, SPECT, and PET scans revealed a similar accuracy of 80%, 85%, and 85%, respectively ($P = .247$). Exclusion of moderate and poor-quality scans resulted in a high and comparable diagnostic performance of CCTA, SPECT and PET for the diagnosis of significant CAD. The authors concluded that the diagnostic value of CCTA and SPECT was hampered by scan quality, while PET seemed not to be affected by scan quality.

Chaudhry et al¹⁰ investigated radionuclide molecular imaging of apoptosis in heart transplant rejection. Apoptosis is a hallmark of transplant rejection. The authors non-invasively targeted cell-mediated apoptotic rejection with the novel SPECT/CT imaging agent, ^{99m}Tc-duramycin (^{99m}Tc-D). In a 19 B6 mice received abdominal heterotopic cardiac allografts, the authors measured activity in a region of interest (ROI) and calculated percent injected dose per gram (%ID/g) in heterotopic and native hearts. Rejection was graded using the International Society of Heart and Lung Transplantation (ISHLT) rubric. Mean ROI and %ID/g was greater in allogeneic animals as compared to control animals ($P = .012$ and $P = .005$, respectively). Mean ROI difference was significantly greater in allogeneic animals as compared to immunosuppressed animals ($P = .021$). Uptake was significantly correlated with ISHLT-graded severity of rejection ($P = .002$). The authors concluded that ^{99m}Tc-D is a feasible tracer to delineate heart transplant rejection non-invasively.

PET

At AHA2018, several studies were presented that focused on positron emission tomography (PET) and its role in clinical cardiology.

PET-derived myocardial blood flow (MBF) utilization in everyday clinical practice and how it can guide clinical decision making received special attention. Patel and colleagues from Mid America Heart Institute attempted to use PET MBF to identify patients whose angina and health status would improve with revascularization. They performed a sub analysis of the ASPIRE study which enrolled 323 symptomatic patients with known CAD who underwent rubidium-82 PET myocardial perfusion imaging (MPI) and followed prospectively for 12 months. In this cohort, 28% had diabetes and 15% had revascularization after PET. In adjusted analysis, there was a significant interaction between ischemia (sum difference score or SDS) and revascularization ($P = .03$ for quality of life), such that patients with $SDS \geq 6$ had greater odds of improvement at 12 months (i.e., less angina, better health status). Interestingly, revascularization in those with $SDS < 6$ had no improvement in angina and quality of life with revascularization.¹¹ It is important to note that many of those patients with moderate to severe ischemia were not referred to coronary angiography for various reasons as another abstract indicated. Of the 879 patients with moderate to severe ischemia included, 526 (59.8%) patients were referred to coronary angiography within 90 days while 353 (40.2%) patients were treated conservatively with medical therapy (Figure 2).¹²

Coronary artery calcium (CAC) scoring is often performed with PET imaging. A study investigated the incremental value of CAC and MBF in predicting 60-day revascularization in 1504 patients. Global stress MBF, CAC and coronary flow reserve (CFR) predicted 60-day revascularization similarly (AUC = 0.72, 0.69, 0.71). CAC and stress MBF were both independently associated with revascularization, (P value $< .0001$). Thus, global stress MBF combined with CAC are predictive of the need for subsequent revascularization.¹³

Patel and colleagues also presented in the young investigator award competition on whether myocardial blood flow reserve (MBFR) can identify patients who have a survival benefit with early revascularization as compared to medical management. The study included a large cohort of 12,594 consecutive patients who underwent rubidium-82 rest/stress PET MPI. Patients with known cardiomyopathy (LVEF $< 40\%$), prior CABG, and missing MBFR measurements were excluded. Rest and Stress absolute MBF were calculated using the net-retention model. After a median follow-up of 3.2 years, 897 patients (7.1%) had early revascularization and 1699 patients (13.5%) experienced all-cause mortality. There was a significant interaction between MBFR and early revascularization ($P = .001$) such that patients with $MBFR \leq 1.8$ had a survival benefit with early

revascularization [HR = 0.76 (0.62, 0.94)], while those with MBFR > 1.8 had higher mortality with revascularization [HR = 1.39 (1.01, 1.94)].¹⁴

Al-Mallah et al looked at whether non-invasive hyperemic myocardial blood flow (HMBF) in patients with suspected or known CAD adds incremental prognostic value over clinical variables. They included 5770 consecutive patients (mean age 61 ± 12 years, 45% females) who underwent rubidium-82 rest/stress positron emission tomography for clinical indications. Patients were followed up for a median duration of 2.2 years for incident cardiac death or myocardial infarction (CD/MI). A total of 32% of the patients had evidence of perfusion defects. Over the follow-up period, A total of 290 (5%) patients developed CD/MI (8.7% in those with HMBF below 2.6 mL/g/min. vs 1.1% in the other group, $0 < 0.0001$). In multivariate analysis, Both HMBF (HR 0.38, 95% CI 0.31-0.45, $P < .0001$) and CFR (HR 0.67, 95% CI 0.58-0.67, $P < .0001$) were independently associated with increased risk of CD/MI (95% confidence interval, 3.1-6.1 $P < .0001$). HMBF improved model discrimination over CFR (Area under the curve increased from 0.822 to 0.837, $P = .014$).¹⁵

The role of PET in hybrid imaging was also discussed at AHA 2018. Several abstracts looked at PET/CT and PET/CMR applications. A study for the national Institute of Health showed that in psoriasis patients, the presence of high-risk plaque on CCTA was associated with higher Amygdala Activity (Odds ratio [Confidence Interval]: 3.33 [1.41-7.84]). This remained significant independent of cardiovascular risk factors, statin use, and psoriasis therapy (2.65 [1.01-6.91]). Thus, neurobiological mechanisms related to chronic psychosocial stress, may play a role in inflammatory atherogenesis.¹⁶

Another study looked at the feasibility of utilizing continuous ¹⁸F-fluorodeoxyglucose infusion in human subjects to assess real-time response to cardiac stressors. Using PET/CMR, subjects underwent standard CMR while receiving continuous FDG infusion for 60 minutes, with the first 15 minutes in normoxia (FiO₂ = 0.209) followed by 45 minutes in hypoxia (FiO₂ = 0.12). Hypoxia resulted in expected non-significant hemodynamic change. While skeletal muscle and liver showed significant decreases in glucose uptake during hypoxia, the myocardium did not demonstrate a significant shift in activity. Thus, real-time cardiac contractile activity and metabolism could be imaged using simultaneous PET/CMR with continuous FDG infusion captures.¹⁷

COMPUTED TOMOGRAPHY

Multiple studies were presented at AHA 2018 studied the role of CCTA and CAC score in clinical practice.

A study examined the role of CAC score in patients taking statins. From the Coronary Artery Calcium Consortium, 6815 patients who were taking statin were studied for cardiovascular disease (CVD) mortality. During the follow-up period, 140 participants died of CVD. One unit increase in log CAC score was associated with significantly increased risk of CVD mortality (hazard ratio (HR), 1.09; 95% CI 1.07-1.11). Compared to CAC = 0, those with CAC score ≥ 400 had 2.5-fold increased risk. Thus, CAC scores remain a strong predictor of CVD mortality even among asymptomatic patients who are taking statin.¹⁸

Most of the clinical recommendations in guidelines suggest using estimates of pre-test likelihood as a prerequisite to determine the need for further testing and the choice of testing. However, these tools were developed many years ago using older cohorts and may not represent the current clinical populations. A study for the National Institute of Health attempted to externally validate prediction models for obstructive CAD in a contemporary, real world population. It included 727 symptomatic subjects (age 40-90 years without known CAD) referred for CAD evaluation underwent CAC and CCTA. Obstructive CAD was defined as $\geq 50\%$ stenosis on CCTA. Pre-test probabilities for obstructive CAD were calculated using modified Diamond-Forrester and other scores. C-statistics for the modified Diamond-Forrester 0.677 (95% confidence interval: 0.617-0.734), and for a basic clinical model 0.723 (0.669-0.774), and for an extended model 0.851 (0.813-0.886). Thus, this study showed that the modified Diamond-Forrester has limited predictability in contemporary cohorts and newer models should be developed and adopted to identify patients needing further non-invasive and invasive testing.¹⁹ This was confirmed in the PROMISE trial which showed that using a new pre-test probability (PTP) score derived from the PROMISE cohort would have reclassified 50.2% (2152/4284) patients from the intermediate (PTP 15-85%) to low PTP/no-testing group (PTP < 15%). This is important since in the PROMISE trial, 164 (7.6%) underwent angiography in the CCTA arm of which only 65 (3.0%) underwent coronary revascularization.²⁰

In addition, prediction of progression of CAD on CCTA using machine learning techniques was highlighted in an abstract from the PARADIGM study.²¹ It included 1255 patients (mean age: 60, 712 (57%) male) who underwent repeated CCTA. Quantitative CT plaque analysis was performed and rapid plaque progression

was defined as annual progression of percent plaque volume more than estimated cut-off (0.48%/year). Using machine learning, a total 82 variables were studied, of which ten were considered to be the most important. These ten variables were primarily related to the baseline plaque volume, type and characteristics as well as other plaque high-risk features. The machine learning model exhibited a higher performance to predict rapid plaque progression (Model: 0.84 (95% CI 0.80-0.88))

Another abstract studied a newly suggested new high-risk feature in CCTA that is adipocyte lipid content, peri-coronary adipose tissue (PCAT) CT attenuation. A study of 111 stable patients with CAD (age 59.2 ± 9.8 years, male 76%) who underwent sequential CTA with the same acquisition protocol (3.4 ± 1.6 years apart) was presented. Goeller et al performed detailed plaque analysis including plaque volume, type and attenuation using semi-automated software. PCAT CT attenuation (HU) was measured in 3D layers around the proximal segment of the right coronary artery. Patients with an increase of non-calcified plaque (NCP) burden showed an increase of PCAT CT attenuation, whereas patients with a decrease of NCP burden showed a decrease of PCAT CT attenuation (4.4 HU vs -2.78 HU, $P < .0001$). In multivariable analysis, only baseline PCAT CT attenuation (Odds Ratio (OR) 1.32, 95% CI 1.03-1.68; $P = .029$) and its change (OR 2.39, 95% CI 1.6-3.5; $P < .001$) were independently related to an increase in NCP burden. This analysis suggested that PCAT CT attenuation may potentially help to identify coronary arteries at increased risk of plaque progression derived from routine CTA.²²

The assessment of patients with intermediate coronary lesions on CCTA is still controversial. There were few abstracts at the meeting looking at the role of CCTA based fractional flow reserve (CT-FFR) in these patients. A study investigated the diagnostic accuracy of CT-FFR using a new method that has the potential to be performed onsite (fluid structure interactions) for CAD compared with CCTA. A total of 174 major vessels in 64 patients were enrolled. Overall, the sensitivity, specificity, and accuracy of CCTA and CT-FFR to detect CAD were 96%, 71% and 75% vs 92%, 83%* and 85%* ($*P < .05$), respectively.²³ There was no significant difference of the diagnostic accuracy for the detection of obstructive CAD between CCTA and CT-FFR in the mild and moderate CAC groups. In the severe CAC group, the sensitivity, specificity, accuracy, positive predict value and negative predict value of CCTA and CT-FFR were 94%, 37%, 56%, 42% and 93% vs 94%, 69%*, 77%*, 59%* and 96% ($*P < .05$), respectively.²⁴ The same group also tested another solution utilizing deep learning in 119 patients of which 53% had abnormal invasive FFR. The deep-learning

FFR achieved area under the receiver-operating characteristic curve of 0.78 for detection of abnormal FFR; and was significantly higher than for CCTA > 50% stenosis (AUC = 0.57). The deep-learning FFR model achieved 73.1% accuracy for detecting abnormal invasive FFR, with sensitivity of 86.6% and specificity of 60.0%.²⁵ Thus, it appears that new tools are on the horizon, but will need more time for further adjustments, fine tuning and calibration.

CARDIAC MAGNETIC RESONANCE IMAGING

We summarize some of the key abstracts presented in the 2018 AHA Scientific Sessions relating to Cardiovascular Magnetic Resonance (CMR).

CMR has long been utilized to evaluate cardiac sarcoidosis. Kazmirczak et al²⁶ evaluated what specific features of CMR late gadolinium enhancement (LGE) are associated with increased risk of cardiac sarcoidosis related major adverse cardiovascular outcomes. They did this by identifying pathologic findings from excised hearts (from transplant recipients or autopsy) and then evaluating for corresponding CMR LGE features in a group of patients with suspected cardiac sarcoidosis. The high-risk group from histologic examination had abnormal features in the epicardium, or multifocal or septal abnormalities. They found that in 286 patients, 85 (30%) had LGE, and the high-risk phenotype was found in 29% of these with higher cardiac sarcoidosis related major adverse cardiovascular outcomes and all-cause death. Those with LGE but without the high-risk phenotype had similar event free survival as those without LGE. More extensive LGE corresponded to a higher hazard ratio (HR 1.07 for every 1% increase in LGE extent, $P = .03$). Thus, this specific LGE pattern in cardiac sarcoidosis may help identify those at highest risk.

In another paper by the same group focusing on LGE in cardiac sarcoidosis patients, the authors examined 52 patients with suspected cardiac sarcoidosis who had both CMR and endomyocardial biopsy, using an automated threshold method to determine areas and extent of LGE, including separately analyzing the LGE on the right ventricle side of the septum.²⁷ 9 of the patients (17%) had non-caseating granulomas, and on parametric evaluation of the test performance, it was found that a cut-off of > 14.7% of LGE on the right ventricular side of the septum yielded a 100% sensitivity and 79% specificity for predicting a positive endomyocardial biopsy. Based on these data, the CMR with LGE can help identify those in whom a cardiac biopsy may be useful.

CMR with LGE offers a non-invasive means to evaluate for fibrosis in hypertrophic cardiomyopathy and

is often used for this purpose, but the rate of fibrotic development is not known. Habib et al²⁸ examined 150 hypertrophic cardiomyopathy patients who had two CMR examinations, separated by an interval of 4.7 ± 1.8 years. In the baseline CMR, only 65% had LGE, which increased to 84% in the second exam. 23% of patients had no progression, 27% had progression of less than 1 g, and 50% had progression > 1 g. On average, the extent of LGE increased by 0.58 ± 1.92 g/year. Higher progression rates were seen in those with lower initial LGE, and in the apical hypertrophic cardiomyopathy variants and these factors were significant predictors of high progression in a multivariate analysis ($P < .001$). Rates of hypertrophic cardiomyopathy related adverse events were associated with baseline exam extent of LGE, but not with progression rates. This provides another means by which CMR can be used to understand the natural history of fibrosis in hypertrophic cardiomyopathy.

Heart failure subgroups may be classified into those with reduced LVEF (HFrEF, LVEF $< 40\%$), preserved EF (HFpEF, LVEF $> 50\%$), and more recently the moderately reduced EF group (HFmEF, LVEF 40 to 50%). The HFmEF group is not as well characterized as the other groups in terms of pathologic and specific imaging findings. Doeblin et al²⁹ investigated 13 patients with HFrEF, 14 patients with HFmEF, and 13 patients with HFpEF with CMR with LGE, including native T1 mapping and extracellular volume (ECV) and T2 mapping. ECV, native T1, and T2 values were significantly higher in HFmEF than in HFpEF and were close in value to those of HFrEF. The authors hypothesize that based on these findings, treatment for HFmEF might be more effective if the strategy is more similar to that used for HFrEF.

Patients presenting with elevated cardiac troponin in the setting of chest pain, but with non-obstructed coronary arteries on angiography, is a common clinical problem in which optimal treatment is often unclear since the exact cause of the myocardial necrosis may not be known. CMR can help distinguish the etiology of the biomarker elevation and provide information useful for treatment. Bhatia et al³⁰ examined 215 patients in a retrospective fashion, over a 16 year period, who had elevated cardiac troponin-T, and underwent coronary angiogram within 30 days of the elevation, with findings of no significant obstruction, and had CMR within 30 days of the elevation. Depending on the CMR results, they were classified as having myocarditis (in 32%), small territory infarction (in 22%), non-ischemic cardiomyopathy (in 20%), stress cardiomyopathy (in 9%), or normal (in 17%). Those with small territory infarction were likely to be placed on medical therapy for ischemic heart disease. At 5 year follow-up, there were no

differences in major adverse cardiovascular events or death between any of the groups. While the specific type of injury did not seem to affect prognosis, it did allow for customization of the treatment strategy.

Global CFR can be assessed by the increase in flow in the coronary sinus following infusion of vasodilator using a phase contrast velocity mapping technique and is a simple, quantitative measure. The prognostic value of CMR-derived CFR is unknown, though the value from PET measurement is known to be useful. Evans et al³¹ evaluated 507 patients undergoing Regadenoson stress perfusion CMR and calculated CFR as the ratio of stress:baseline coronary sinus flow. They were followed longitudinally for outcomes of death, non-fatal myocardial infarction, heart failure hospitalization, sustained ventricular tachycardia, and late revascularization. Over a 2.1 year follow-up, 80 patients experienced an event, with log-rank P value $< .001$ for increased risk in those with CFR less than the median of 2.2. This held up after adjustment for clinical and imaging risk factors of ischemia, LVEF, and LGE. Thus, this simple-to-perform measure provides useful prognostic information in patients undergoing regadenoson stress perfusion CMR.

ECHOCARDIOGRAPHY

Many exciting abstracts in echocardiography have been presented at the AHA 2018 Scientific Sessions. We summarize here a selection of these abstracts.

CAD is a leading cause of morbidity and mortality. Post-acute myocardial infarction and immediately after percutaneous revascularization, 3-dimensional global longitudinal strain was an independent predictor of final infarct size and left ventricular remodeling, particularly when combined with E/e' , a marker of filling pressures and diastolic dysfunction.³² While many patients post-infarction have apparent preserved ejection fraction, particularly if the infarct is small or revascularization was performed in a timely manner, this may not be the most robust marker of left ventricular systolic dysfunction. Indeed, Iwakura et al³³ showed that among patients two weeks post myocardial infarction with ejection fraction $\geq 50\%$, less than 20% had normal global longitudinal strain (-20%), and that those with impaired strain had increased mortality ($P = .048$). Hence strain analysis should be an integral component of left ventricular systolic function assessment in this setting.

Diastolic dysfunction is also well recognized to be associated with increased morbidity and mortality, particularly as it progresses with time.³⁴ Ozbek et al³⁵ showed that E/e' provides incremental prognostic value (hazard ratio 1.08, 95% CI 1.01-1.15, $P = .021$, per 1

increase) among diabetic patients and is a stronger predictor of outcomes than in non-diabetic patients.

The new American Society of Echocardiography guidelines for grading diastolic dysfunction however, have resulted in many patients being assigned to the “indeterminate” category.³⁶ While many parameters are integrated in the assessment of diastolic function, Tsujishi et al³⁷ assessed the role of left atrial strain with three-dimensional speckle tracking analysis in 241 patients. They found that the worse the diastolic function, the lower the left atrial strain. Left atrial strain had the highest area under the curve to distinguish diastolic dysfunction. Moreover, left atrial strain was able to classify the diastolic function of all patients previously categorized as indeterminate (9%). Furthermore, left atrial strain outperformed traditional echocardiographic parameters, and proved to be an accurate non-invasive tool with good correlation with invasive catheterization in the assessment of diastolic function, particularly among patients with heart failure and preserved ejection fraction.³⁸ In addition to identifying and classifying patients with diastolic dysfunction, left atrial strain carries prognostic value. Indeed, among patients with heart failure and reduced ejection fraction undergoing resynchronization, left atrial strain predicted outcomes (death, left ventricular assist device, or transplantation), and added incremental value beyond traditional covariates including left atrial volume index and global left ventricular longitudinal strain.³⁹

Other parameters of diastolic dysfunction such as time constant of LV pressure decline (Tau), end-diastolic pressure and end-diastolic stress, have also been successfully measured and quantified non-invasively using real-time one-beat 3-dimensional speckle tracking echocardiography with high volume rate, and showed moderate correlation to the invasively measured parameters with catheterization.⁴⁰ Increased epicardial adipose tissue is associated with inflammation that is a precursor to atherosclerosis and diastolic dysfunction. Utsunomiya et al⁴¹ showed that among patients with calcium score of zero, increased epicardial fat was associated with a decrease of early diastolic mitral annular velocity; hence, a potential new marker of diastolic dysfunction in the preclinical phase of CAD.

The assessment of systolic pulmonary artery pressure using maximum tricuspid regurgitation velocity is often underestimated when the jet signal is suboptimal. The administration of agitated saline or contrast enhanced Doppler signal yielded more accurate estimates of systolic pulmonary artery pressure vs unenhanced echocardiograms as compared to invasive measurements.⁴² Among patients with pulmonary hypertension ($n = 575$), impaired right ventricular systolic function, particularly longitudinal systolic strain, is

associated with increased mortality (hazard ratio 1.4, 95% CI 1.2-1.6, $P < .0001$, per 5% decline in right ventricular strain). On follow-up echocardiogram ($n = 217$), those with persistently moderately impaired or with worsening of right ventricular strain had 5.1-fold increased risk of death.⁴³ Sudden cardiac death is thought to be a major cause of death among patients with right ventricular systolic dysfunction. Indeed, in a community based study, Pandat et al⁴⁴ showed that reduced fractional area contraction, a known marker of right ventricular systolic dysfunction, is associated with increased odds of sudden cardiac death (odds ratio 1.14, 95% CI 1.04-1.25, $P = .005$, per 5% decrease). Furthermore, among patients undergoing left side valvular surgery, pre-operative right ventricular systolic dysfunction is an independent predictor of 30 days post-operative complications (odds ratio 2.92 [1.46-5.8] for aortic valve surgery, and 2.2 [1.08-4.6] for mitral valve surgery, $P < .05$ for both).⁴⁵

Zhang et al mapped the left atrial appendage orifice perimeter in 21 patients undergoing transesophageal echocardiography prior to left atrial appendage closure device implantation. Three-dimensional volumetric data acquisition was performed with subsequent 3-D model printing of the left atrial appendage. This 3-D model correlated well with the size of the device closure used, and could guide optimal size selection and procedure planning.⁴⁶ Three-dimensional echocardiography models of the heart valves can also be fused with computed tomography anatomical images of the heart resulting in a hybrid 3-D model with comprehensive data.⁴⁷

With the evolution of technology, hand-held echocardiography is becoming prominent and an integral part of bedside examination. Unfortunately, with the advancement in technology fewer physicians are proficient at cardiac auscultation. Stanger demonstrated that hand-held echocardiography is superior to auscultation in identifying regurgitant valvular disease. However, auscultation remains superior to hand-held echocardiography for assessment of aortic stenosis.⁴⁸ Also, physicians often rely on the cardiology fellow on-call to perform echocardiograms, particularly after hours. In a prospective study, Yang et al⁴⁹ showed that first-year cardiology fellows performance and interpretation of echocardiograms carries major clinically significant discordance with attending reading of more than 4% of cases.

Disclosures

Drs. Al-Mallah, Lloyd and Aljaroudi report no conflicts of interest. Dr. Doukky reports research grant support from Astellas Pharma (Northbrook, IL). Dr. Hage reports research grant support from Astellas Pharma and GE Healthcare.

References

1. AlJaroudi WA, Lloyd SG, Hage FG. Multi-modality imaging: Bird's eye view from the 2017 American Heart Association Scientific Sessions. *J Nucl Cardiol* 2018;25:678-84.
2. AlJaroudi WA, Lloyd SG, Chaudhry FA, Hage FG. Multi-modality imaging: Bird's eye view from the 2016 American Heart Association Scientific Sessions. *J Nucl Cardiol* 2017;24:946-51.
3. Einstein AJ, Lloyd SG, Chaudhry FA, AlJaroudi WA, Hage FG. Multi-modality Imaging: Bird's eye view from the 2015 American Heart Association Scientific Sessions. *J Nucl Cardiol* 2016;23:235-43.
4. AlJaroudi WA, Einstein AJ, Chaudhry FA, Lloyd SG, Hage FG. Multi-modality imaging: Bird's-eye view from the 2014 American Heart Association Scientific Sessions. *J Nucl Cardiol* 2015;22:364-71.
5. Saito Y, Arimoto T, Kutsuzawa D, Yokoyoma M, Tsuchiya H, Takahashi H, et al. The association between cardiac sympathetic nervous function and cardiac rehabilitation responder. *Circulation* 2018;138:A10880.
6. Cantu S, Berman DS, Hayes SW, Friedman J, Azarbal B. Association of exercise capacity, heart rate recovery, chronotropic incompetence and all-cause mortality during exercise-myocardial perfusion single-photon emission computerized tomography in patients with left ventricular systolic Dysfunction. *Circulation* 2018;138:A14437.
7. Al Badarin F, Spertus JA, Chan PC, Patel KK, Kennedy KF, Bateman TM. Differences in post-test invasive angiography referral patterns between PET and SPECT. *Circulation* 2018;138:A11080.
8. AlMallah M, Masoudi F, Ebid M, Ahmed A. SPECT myocardial perfusion imaging adds incremental prognostic value over cardiorespiratory fitness. *Circulation* 2018;138:A11555.
9. van Diemen P, Driessen RS, Stuijzfand WJ, Raijmakers PJ, Schumacher SP, Min JK, et al. The impact of scan quality on the diagnostic performance of CCTA, SPECT and PET for Diagnosing myocardial ischemia as defined by fractional flow reserve: A PACIFIC-trial substudy. *Circulation* 2018;138:A14778.
10. Chaudhry F, Adapoe MK, Johnson KW, Petrov A, Chaudhry FF, Pak KY, et al. Nuclear molecular imaging of apoptosis in heart transplant rejection. *Circulation* 2018;138:A16168.
11. Patel KK, Badarin FA, Spertus JA, Chan PS, Arnold SV, Kennedy KF, et al. Abstract 12566: Ischemia on positron emission tomography (PET) myocardial perfusion imaging (MPI) identifies patients with improvement in angina and health status post-revascularization. *Circulation* 2018;138:A12566.
12. AlMallah MH, Masoudi F, Ahmed A, Aljizeeri A. Abstract 11557: Referral to coronary angiography among patients with moderate or severe ischemia: Implications for the ISCHEMIA trial. *Circulation* 2018;138:A11557.
13. McCubrey RO, Min DB, Meredith KG, Biswas S, Knight S, Mason SM, et al. Abstract 11540: Predictive ability of cac and myocardial blood flow: In a real world setting. *Circulation* 2018;138:A11540.
14. Patel KK, Spertus JA, Chan PS, Badarin FA, Kennedy KF, Sperry BW, et al. Abstract 11237: Myocardial blood flow reserve assessed by positron emission tomography myocardial perfusion imaging identifies patients with a survival benefit from early revascularization. *Circulation* 2018;138:A11237.
15. AlMallah MH, Ahmed A, Alfariis M, Ahmed D, Suleiman I, Aljizeeri A. Abstract 11553: Incremental prognostic value of positron emission tomography derived hyperemic myocardial blood flow: Comparison with coronary flow reserve. *Circulation* 2018;138:A11553.
16. Dey AK, Goyal A, Elnabawi Y, Chaturvedi A, Chung JH, Aberra T, et al. Abstract 12603: Increased Resting amygdala activity relates to increased prevalence of high risk coronary plaque in psoriasis. *Circulation* 2018;138:A12603.
17. Razalan MGF, Centanni R, Barton GP, McMillan AB, Goss KN. Abstract 16689: Simultaneous assessment of cardiac metabolism and function using PET/MR with continuous FDG infusion. *Circulation* 2018;138:A16689.
18. Mirbolouk H, Charkhchi P, Uddin SMI, Orimoloye OA, Shaw L, Berman DS, et al. Abstract 16618: Prognostic significance of coronary artery calcium (CAC) score among patients on statin therapy: Results of coronary artery calcium consortium, a multi-center cohort study. *Circulation* 2018;138:A16618A.
19. Hu-Wang E, Kureshi F, Leifer ES, Acharya T, Sathya B, Yu JH, et al. Abstract 12022: Calcium scoring improves pretest probability estimation of obstructive coronary artery disease in a real world population. *Circulation* 2018;138:A12022.
20. Foldyna B, Udelson JE, Karady J, Banerji D, Lu MT, Mayrhofer T, et al. Abstract 16375: Potential downstream effects of replacing diamond-forrester with observed contemporary prevalence of obstructive CAD: The promise trial. *Circulation* 2018;138:A16375.
21. Han D, Kolli KK, Gransar H, Lin FY, Lee JH, Rizvi A, et al. Abstract 15831: Novel prediction model based on machine learning algorithm to identify rapid coronary plaque progressor using quantitative assessment of coronary computed tomography angiography. *Circulation* 2018;138:A15831.
22. Goeller M, Tamarappoo Balaji K, Kwan Alan C, Otaki Y, Cadet S, Commandeur F, et al. Abstract 15929: Relationship between changes in pericoronary adipose tissue attenuation and plaque progression by coronary CTA. *Circulation* 2018;138:A15929.
23. Yamauchi Y, Kanzaki Y, Ozeki M, Fujisaka T, Takeda Y, Morita H, et al. Abstract 11110: Diagnostic accuracy of on-site CT-fractional flow reserve (CT-FFR) to detect coronary artery disease. *Circulation* 2018;138:A11110.
24. Yamauchi Y, Kanzaki Y, Ozeki M, Fujisaka T, Takeda Y, Morita H, et al. Abstract 11173: feasibility of novel on-site operated CT-fractional flow reserve (CT-FFR) to detect of coronary artery disease in patients with severe coronary artery calcification. *Circulation* 2018;138:A11173.
25. Kawaguchi YO, Fujimoto S, Kumamaru KK, Otsuka Y, Kato E, Aoshima C, et al. Abstract 12206: Fully automated 3D deep-learning analysis of coronary CT Angiography: Prediction of fractional flow reserve. *Circulation* 2018;138:A12206.
26. Kazmirczak F, Chen K, Okasha O, Farzaneh-Far A, Duval S, von Wald L, et al. Rapid visual pathology-based late gadolinium enhancement phenotyping on cardiovascular magnetic resonance imaging improves risk stratification of patients with suspected cardiac sarcoidosis. *Circulation* 2018;138:A15984.
27. Chen K, Kazmirczak F, Okasha O, Farzaneh-Far A, Shenoy C. Late gadolinium enhancement cardiovascular magnetic resonance imaging characteristics predict the yield of endomyocardial biopsy in patients with suspected cardiac sarcoidosis. *Circulation* 2018;138:A17337.
28. Habib M, Adler A, Fardini K, Hanneman K, Rowin E, Maron M, et al. Progression of myocardial fibrosis in hypertrophic cardiomyopathy: A cardiac magnetic resonance study. *Circulation* 2018;138:A13069.
29. Doebelin PJ, Pieske B, Kelle S, Gebker R, Lapinskas T, Edelmann F, et al. HFmEF differs from hpfef and hrfef in advanced cmr imaging markers of adverse cardiac remodeling. *Circulation* 2018;138:A13417.
30. Bhatia S, Jaffe A, Gersh B, Chandrasekaran K, Anstine C, Anavekar N. Spectrum of disease and outcomes of troponin positive,

- angiogram negative patients assessed by cardiac MRI. *Circulation* 2018;138:A12156.
31. Evans KL, Indorkar R, Kwong R, Romano S, White BE, Chia RC, et al. Global coronary flow reserve measured during stress cardiac magnetic resonance imaging is an independent predictor of adverse cardiovascular events. *Circulation* 2018;138:A12903.
 32. Iwahashi N, Takahashi A, Akiyama E, Okada K, Matsuzawa Y, Konishi M, et al. Global strain estimated by 3D speckle tracking combined with E/E' is the strongest predictor in patients with STEMI. *Circulation* 2018;138:A12462.
 33. Iwakura K, Okamura A, Koyama Y, Inoue K, Iwamoto M, Nagai H, et al. Impaired global longitudinal strain is associated with poor prognosis even in patients with preserved ejection fraction after myocardial infarction. *Circulation* 2018;138:A13236.
 34. Aljaroudi W, Alraies MC, Halley C, Rodriguez L, Grimm RA, Thomas JD, et al. Impact of progression of diastolic dysfunction on mortality in patients with normal ejection fraction. *Circulation* 2012;125:782-8.
 35. Ozbec BT. Diastolic dysfunction is a stronger predictor of cardiovascular morbidity and mortality in individuals with diabetes as compared to individuals without diabetes in the general population. *Circulation* 2018;138:A12554.
 36. Nagueh SF, Smiseth OA, Appleton CP, Byrd BF 3rd, Dokainish H, Edvardsen T, et al. Recommendations for the evaluation of left ventricular diastolic function by echocardiography: an Update from the American Society of Echocardiography and the European Association of Cardiovascular Imaging. *J Am Soc Echocardiogr* 2016;29:277-314.
 37. Tsujiuchi M, Ebato M, Maezawa H, Nogi A, Mizukami T, Nagumo S, et al. Categorization of left ventricular diastolic dysfunction using left atrial strains calculated by three dimensional speckle tracking analysis. *Circulation* 2018;138:A12863.
 38. Kawamura I, Tanaka R, Yoshizane T, Minatoguchi S, Sato H, Ono K, et al. Novel and noninvasive evaluation of left ventricular diastolic dysfunction in patients with normal ejection fraction using 3-dimensional speckle echocardiography. *Circulation* 2018;138:A11143.
 39. Kagiya N, Sugahar M, Soyama Y, Adelstein E, Gorcsan J. Left atrial strain has additive prognostic value to left ventricle global longitudinal strain in patients receiving cardiac resynchronization therapy. *Circulation* 2018;138:A13227.
 40. Kawamura I, Tanaka R, Yoshizane T, Minatoguchi S, Saeki M, Nagaya M, et al. Noninvasive evaluation of left ventricular systolic and diastolic properties in hypertension using real-time one-beat 3-dimensional speckle tracking echocardiography with high volume rate. *Circulation* 2018;138:A11116.
 41. Utsunomiya H, Yamamoto H, Shimada A, Kitagawa T, Hidaka T, Kihara Y. Increased epicardial adipose tissue volume is associated with left ventricular diastolic function in patients with zero coronary artery calcium score. *Circulation* 2018;138:A17402.
 42. Lee L, Kinno M, Schultz R, Kane B, Cascino G, Maganti K. Use of contrast-enhanced echocardiography for evaluating pulmonary artery pressure. *Circulation* 2018;138:A17391.
 43. Lekhakul A, Fine N, Chen L, Kane GC. Right ventricular longitudinal systolic strain for prediction of long-term mortality in patients with pulmonary hypertension. *Circulation* 2018;138:A13089.
 44. Pandat S, Nagaura T, Nair S, Reinier K, Uy-Evanado A, Rusinaru C, et al. An association between right ventricular dysfunction and sudden cardiac death. *Circulation* 2018;138:A12624.
 45. Towheed A, Sabbagh E, Assiri SA, Chowdhury MA, Moukarbel GV, Schwann T, et al. Association of right ventricular dysfunction by echocardiographic parameters with short term adverse outcomes after left sided valvular surgery. *Circulation* 2018;138:A12165.
 46. Zhang B, Jia D, Song H, Zhang L, Mei D. Measurement of left atrial appendage orifice perimeter using echocardiographic 3D printed model for the guidance of LAmbré™ Occluder selection. *Circulation* 2018;138:A10539.
 47. Zhang B, Chen S, Yang Y, Jia D, Zhou Q. Preliminary precision study of 3D printing heart model by multimodal medical image fusion technology. *Circulation* 2018;138:A10540.
 48. Stanger D. Insonation vs auscultation in valvular disorders: Is aortic stenosis the exception? *Circulation* 2018;138:A10943.
 49. Yang J, Spahillari A, McCormick I, Quinn G, Manning W. On-call transthoracic echocardiographic interpretation by first year cardiology fellows: Comparison with attending cardiologists. *Circulation* 2018;138:A10780.

Publisher's Note Springer Nature remains neutral with regard to jurisdictional claims in published maps and institutional affiliations.